BAREKENG: Journal of Mathematics and Its Applications
June 2025 Volume 19 Issue 2 Page 0937–0948
P-ISSN: 1978-7227 E-ISSN: 2615-3017
https://doi.org/10.30598/barekengvol19iss2pp0937-0948

ESTIMATING EARTHQUAKE MAGNITUDE USING SPATIAL INTERPOLATION WITH THE INVERSE DISTANCE WEIGHTING AND ORDINARY KRIGING APPROACH

Fitri Amalia[1], Achmad Fauzan[2*]

[1,2]Statistics Study Program, Faculty of Mathematics and Natural Sciences, Universitas Islam Indonesia
Jln. Kaliurang KM 14.5, Sleman, Yogyakarta, 55584, Indonesia

*Corresponding author's e-mail: *achmadfauzan@uii.ac.id*

ABSTRACT

The West Java region is known for its high disaster vulnerability, particularly to earthquakes, due to the presence of many active faults. Based on this, information is needed as an initial step for disaster mitigation to reduce disaster risk and guarantee community safety in the West Java region, one of which is by carrying out spatial interpolation. In this study, the Inverse Distance Weighted (IDW) and Ordinary Kriging (OK) methods were used. The research sample included data on earthquake magnitude in West Java within the same coordinate range, from 01 January 2022 to 31 December 2022. This research was conducted to find out a more precise spatial interpolation method in estimating the strength of the earthquake in West Java in 2022. From the OK analysis results, the best theoretical semivariogram model was obtained, namely the Exponential model with nugget, sill and range values of 0.07, 0.12 and 11451 meters. From the results of the IDW analysis, the best power value parameter was obtained, namely 2. This research was conducted to develop a more precise spatial interpolation method for estimating earthquake strength in West Java in 2022. The OK method results indicated that most of the West Java region has the potential for earthquakes with a magnitude of around 1.5 to 4.0, while the IDW method suggested a potential magnitude of around 2.0 to 4.0. The potential for a high-magnitude earthquake is in Kp. Cileuley, Garumukti, Pamulihan District, Garut Regency, West Java. Based on the results of Holdout Cross Validation, the IDW method is the best for estimating earthquake magnitude in West Java, with a MAPE value of 17.8%. The IDW method's estimation of earthquake magnitude is superior to OK, with smaller MAPE and MAE values.

Article History:

Received: 8th August 2024
Revised: 31st January 2025
Accepted: 4th February 2025
Published: 1st April 2025

Keywords:

Earthquake;
Inverse Distance Weighted;
Ordinary Kriging.

How to cite this article:

F. Amalia and A. Fauzan., "ESTIMATING EARTHQUAKE MAGNITUDE USING SPATIAL INTERPOLATION WITH THE INVERSE DISTANCE WEIGHTING AND ORDINARY KRIGING APPROACH," *BAREKENG: J. Math. & App.,* vol. 19, iss. 2, pp. 0937-0948, June, 2025.

Journal homepage: *https://ojs3.unpatti.ac.id/index.php/barekeng/*
Journal e-mail: *barekeng.math@yahoo.com; barekeng.journal@mail.unpatti.ac.id*

Research Article · Open Access

1. INTRODUCTION

Indonesia is an archipelagic country located at the meeting point of three active tectonic, the Eurasian plate; the Indo-Australian plate, and the Pacific plate, forming convergent boundaries [1]. This situation distinguishes Indonesia as an active tectonic area with a high level of seismicity [2]. The western Java region is an earthquake-prone in Indonesia, according to the Center for Volcanology and Geological Disaster Mitigation. Regional maps indicate the presence of numerous active faults on the mainland of West Java, which have the potential to trigger damaging earthquake. West Java has well-known active faults, such as the Cimandiri – Lembang Fault and the Baribis Fault [3]. An earthquake is a tremor or shaking of the Earth's surface caused by the collision of tectonic plates, active fault movements, volcanic activity, or rock collapse [4]. Earthquake incidences are categorized as important problems that can be handled by providing early disaster mitigation education. The arrangement of these disaster mitigation activities can increase community preparedness toward reducing disaster risks and fatalities. Therefore, the importance of awareness of natural disaster preparedness can increase collective knowledge on how to face, protect, and save themselves from disasters [5].

In the era of globalization, developments in all aspects are becoming increasingly rapid because of the sophistication of Geographical Information System (GIS) [6]. Geostatistics has been applied in various fields, including geology. One of the primary objectives of geological research is to predict data for locations that have not been directly observed. Ordinary Kriging (OK) and Inverse Distance Weighting (IDW) are frequently used interpolation methods that are used often. The OK and IDW methods calculates estimated area values by assigning larger weights to the nearest sample values [7]. This study compares stochastic and deterministic interpolation methods. The kriging method is a stochastic spatial interpolation method, while the Inverse Distance Weighted (IDW) method is a deterministic spatial interpolation method [8].

Spatial interpolation offers several significant benefits, particularly in term of estimating values at unmeasured locations and mapping the distribution of spatial phenomena, such as air pollution, mineral content, rainfall, and other geospatial data [9][10]. In addition, interpolation helps optimize sampling strategies and data visualization, as well as facilitate analysis and demonstrate research findings. In the fields of environmental science and public health, interpolation is also valuable for risk analysis, such as tracking the spread of pollution or diseases, enabling quicker and more accurate mitigation efforts [11][12]. Several studies have explored both methods, including soil property mapping in the hilly regions of central Vietnam using OK and Regression Kriging (RK) [13]. Qiao [14] compared OK and Inverse Distance Weighting (IDW) methods for interpolating soil pollution in Beijing, China. Additionally, Kumar [15] conducted research on the spatial variation of soil permeability [15], while Lamammra [16] developed a geostatistical model to estimate mineral resources in the Kieselguhr mining area, in Algeria. Beyond interpolation, Kriging modeling is occasionally employed as a tool for data collection, as demonstrated by Kostopoulou's study, where OK was used to retrieve missing satellite data in coastal management [17].

Based on these various applications, this study be focuses on predicting earthquake distribution data in Indonesia, specifically West Java, which is traversed by an active fault (indicating a high potential for earthquakes). The objectives of this research include mapping areas with potential for both high- and low-magnitude earthquakes using the Ordinary Kriging (OK) and Inverse Distance Weighting (IDW) methods. The expected outcome is to raise awareness in regions identified as having high earthquake magnitude based on the interpolation results.

2. RESEARCH METHODS

2.1 Data Sources and Research Stages

The data used in the research is secondary data retrieved from the official BMKG website, with the following URL, http://repogempa.bmkg.go.id/. This research uses a total of 309 earthquake points. The population used is data on earthquake magnitudes in West Java at coordinates 7,842º S to 5,889º S and 106,337º E to 109,138º E. The research sample used is data on earthquake magnitudes in West Java at coordinates 7,842º S to 5,889º S and 106,337º E to 109,138º E within the period 1 January 2022 to 31 December 2022.

Table 1. Earthquake Magnitude Data in West Java Province in 2022

Date	Time	X (Easting)	Y (Southing)	UTM Zone	Magnitude (M)	Location
01/01/2022	20:39:59	673327.7 mE	9196103 mS	48S	2.4	Java, Indonesia
09/01/2022	17:21:48	658993.6 mE	9202785 mS	48S	2.1	Java, Indonesia
⋮	⋮	⋮	⋮	⋮	⋮	⋮
28/12/2022	00:28:34	758692.7 mE	9259905 mS	48S	2.3	Java, Indonesia
30/12/2022	00:51:21	800367.4 mE	9196607 mS	48S	3	Java, Indonesia

2.2 Ordinary Kriging

Ordinary Kriging is a geostatistical method that utilizes spatial values at sampled locations and variograms that represent the relationship between spatial points to estimate values at unmeasured locations, with the estimation influenced by its proximity to the sampled location [18]. The ordinary kriging method assumes that the average is unknown and the value is constant. This method does not accept trends and outliers. The formula for estimation using the Ordinary Kriging method is as follows [19].

$$\hat{Z}(x) = \sum_{i=1}^{n} w_i\big(z(x_i)\big) \tag{1}$$

$\hat{Z}(x)$ denotes the predicted value of the sample point, w_i denotes the weight that determines the distance between points, and $z(x_i)$ is the value at the sample point. The Equation (1) can be changed to Equation (2) so that the estimate obtained is not biased [20].

$$\begin{pmatrix} \gamma(s_1,s_1) & \cdots & \gamma(s_1,s_n) & 1 \\ \vdots & \ddots & \vdots & \vdots \\ \gamma(s_n,s_1) & \dots & \gamma(s_n,s_n) & 1 \\ 1 & \dots & 1 & 0 \end{pmatrix} \begin{pmatrix} w_1 \\ \vdots \\ w_n \\ \varphi \end{pmatrix} = \begin{pmatrix} \gamma(s_0,s_1) \\ \vdots \\ \gamma(s_0,s_n) \\ 1 \end{pmatrix} \tag{2}$$

Equation (2) can also be written as $\boldsymbol{Aw} = \boldsymbol{b}$ with the value of $\boldsymbol{w}$ obtained based on Equation (3).

$$\boldsymbol{w} = \boldsymbol{A}^{-1}\boldsymbol{b} \tag{3}$$

where $\boldsymbol{A}$ is the covariance matrix of actual observations, $\boldsymbol{w}$ is the weight that determine the distances between points, and $\boldsymbol{b}$ is the covariance matrix of actual and predicted observations.

2.3. Experimental Semivariogram

Before calculating the experimental semivariogram values, tests were carried out to determine the presence or absence of outliers and stationarity. Outliers are observations that are significantly different (extreme) from other observed data. One method to detect outliers is to draw a Boxplot [8]. The main statistical assumption in the Kriging method is the stationarity test, because if the data is stationary then the average and semivariogram are the same at all locations within the data range [21]. Stationarity testing can be conducted by visualizing data in 3 dimensions. Furthermore, the experimental semivariogram function is defined in Equation (4) [22].

$$\boldsymbol{\gamma(h) = \frac{1}{2N(h)} \sum_{i=1}^{N(h)} [z(u_i + h) - z(u_i)]^2} \tag{4}$$

where $\gamma(\mathrm{h})$ is the semivariogram, $\mathrm{N(h)}$ is the total number of sample point pairs with distance h, $\mathrm{z(u_i)}$ is the observed value at location $\mathrm{u_i}$ and $\mathrm{z(u_i + h)}$ is the observed value at location $\mathrm{u_i}$+h. To calculate semivariogram values, many pairs of data are divided into several classes using the Sturges equation as follows [19].

$$\mathbf{k = 1 + 3.3\log n} \tag{5}$$

k denotes the number of classes and n denotes the sample size.

There are three parameters used to calculate the theoretical semivariogram: nugget, sill, and range. Nugget is an approximation of the semivariogram value at a distance around zero. Sill is a semivariogram value that remains constant over an infinite distance, where there is no correlation between samples. Meanwhile, the range is the furthest distance at which the semivariogram reaches the sill, which indicates there is no spatial correlation [23]. This research uses the Spherical, Exponential and Gaussian models.

1. Spherical Model

$$\boldsymbol{\gamma}(\mathbf{h}) = \begin{Bmatrix} \mathbf{C_0} + \mathbf{C}\left[\left(\frac{\mathbf{3h}}{\mathbf{2}\boldsymbol{a}}\right) - \left(\frac{\mathbf{h}}{\mathbf{2}\boldsymbol{a}}\right)^{\mathbf{3}}\right] & \mathbf{for}\ \mathbf{0} < \mathbf{h} \le \boldsymbol{a} \\ \mathbf{C_0} + \mathbf{C} & \mathbf{for}\ \mathbf{h} > \boldsymbol{a} \end{Bmatrix} \tag{6}$$

2. Exponential Model

$$\boldsymbol{\gamma}(\mathbf{h}) = \mathbf{C_0} + \mathbf{C}\left[\mathbf{1} - \mathbf{exp}\left(-\frac{\mathbf{h}}{\boldsymbol{a}}\right)\right] \tag{7}$$

3. Gaussian Model

$$\boldsymbol{\gamma}(\mathbf{h}) = \mathbf{C_0} + \mathbf{C}\left[\mathbf{1} - \mathbf{exp}\left(-\frac{\mathbf{h}}{\boldsymbol{a}}\right)^{\mathbf{2}}\right] \tag{8}$$

h is the spatial distance between sample points, $\mathrm{C_0}$ is the nugget, C is the partial sill/structural variance, $\mathrm{C_0} + \mathrm{C}$ is the sill, and a is the range.

2.4 Inverse Distance Weighting

The Inverse Distance Weighting interpolation method uses several surrounding data points to estimate data at unmeasured locations [24]. The power value in the IDW method determines the influence of input points. Therefore, points that are closer exert a greater influence, resulting in more defined surfaces. The weight used for the average is a derivative function of the distance between the sample point and the interpolated point [25]. The general function for weighting is the inverse of the square of the distance which is formulated as **Equation (9)**.

$$\mathbf{w_i} = \frac{\frac{\mathbf{1}}{\mathbf{d_i}^{\mathbf{p}}}}{\sum_{\mathbf{i=1}}^{\mathbf{n}} \frac{\mathbf{1}}{\mathbf{d_i}^{\mathbf{p}}}} \tag{9}$$

Estimation of the point value uses the following **Equation (10) [26]**.

$$\hat{\boldsymbol{Z}}_{\mathbf{0}} = \sum_{\boldsymbol{i}=\mathbf{1}}^{\boldsymbol{n}} \boldsymbol{w_i}.\boldsymbol{Z_i} \tag{10}$$

$\hat{Z}_0$ is the estimated point value, w_i is the weighting factor at point i, Z_i is the value of the point estimator at i, d_i is the distance between point i and the estimated point, and p is the exponential factor. The Euclidean distance formula is defined **Equation (11) [24]**.

$$\boldsymbol{d_{io}} = \sqrt{(\boldsymbol{x_0} - \boldsymbol{x_i})^2 + (\boldsymbol{y_0} - \boldsymbol{y_i})^2} \tag{11}$$

where x_0, y_0 is the estimated point coordinates, and x_i, y_i is the measured point coordinates.

2.5 Prediction Accuracy

There are several types of accuracy indicators in forecasting that are commonly used, some of which are Root Mean Square Error (RMSE), Mean Absolute Error (MAE), and Mean Absolute Percentage Error (MAPE) [27].

1. Root Mean Square Error (RMSE)

$$\mathbf{RMSE} = \sqrt{\frac{1}{n}\sum_{i=1}^{n}(y_i - \hat{y}_1)^2} \tag{12}$$

y_i is the actual data, $\hat{y}_1$ is the predicted data and n is the number of data.

2. Mean Absolute Error (MAE)

$$\mathbf{MAE} = \frac{1}{n}\sum_{i=1}^{n}|y_i - \hat{y}_1| \tag{13}$$

3. Mean Absolute Percentage Error (MAPE)

$$\mathbf{MAPE} = \frac{1}{n}\sum_{i=1}^{n}\left|\frac{y_i - \hat{y}_1}{y_i}\right| \times 100\% \tag{14}$$

2.6 Research Flow

The research stages begin with data input, specifically the earthquake strength data for the West Java region in 2022. An illustration of the flow diagram can be seen in **Figure 1**.

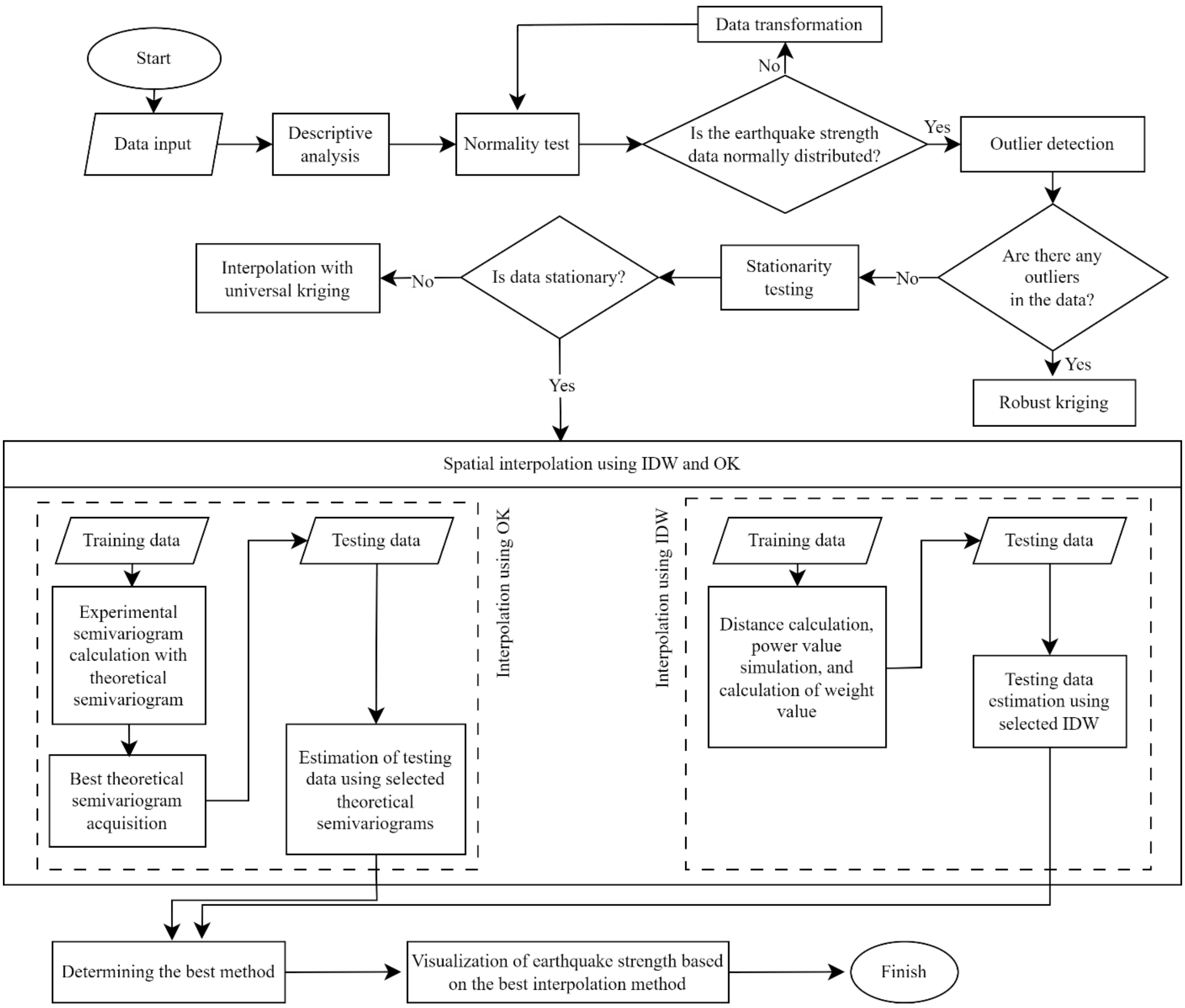

Figure 1. Research Flow Diagram

Based on **Figure 1**, a descriptive analysis is conducted on the collected data to provide a general overview of the dataset. The second step involves testing for normality, stationarity, and outliers. If the data are not normally distributed, transformation can be applied; if the data are non-stationary, universal kriging can be employed; and if the data contain outliers, robust kriging can be utilized. Once these assumptions are met, spatial interpolation is conducted using the IDW and OK methods. Finally, the dataset undergoes Hold-Out Cross-Validation, where it is divided into training and testing subsets.

For the IDW method, the first step is to calculate the Euclidean distance between points. The second step involves running simulations to determine the optimal power value and computing the weights to be used in Equation 9. Once the optimal power is obtained, interpolation is performed across the entire study area to predict unknown values. In the OK method, the initial step is to compute the experimental semivariogram values using Equation 4. The experimental semivariogram is then fitted to an appropriate model based on Equations 6 through 8. The next step is to predict the values at the testing data points. The predictions for the testing data from each method were evaluated using the MAPE, MAE, and RMSE values according to Equations 12 through 14. Upon determining the best method, a comprehensive prediction of the entire region is conducted, followed by visualization of the earthquake the earthquake strength around West Java.

3. RESULTS AND DISCUSSION

3.1 Data Overview

The descriptive statistical analysis describes and presents a comprehensive overview of the analyzed data. **Table 2** presents the descriptive statistics from earthquake magnitude data for West Java in 2022.

Table 2. Descriptive Statistics of 2022 Earthquake Magnitude Data in West Java.

Statistical Measure	Earthquake Magnitude (M)	Focal Depth (km)
Minimum	1.200	5
Mean	2.505	26.8
Median	2.400	12
Maximum	4.300	259

There are a variety of visualization techniques used in descriptive statistical analysis. One method is to visualize the distribution of research data to find out how the data is distributed.

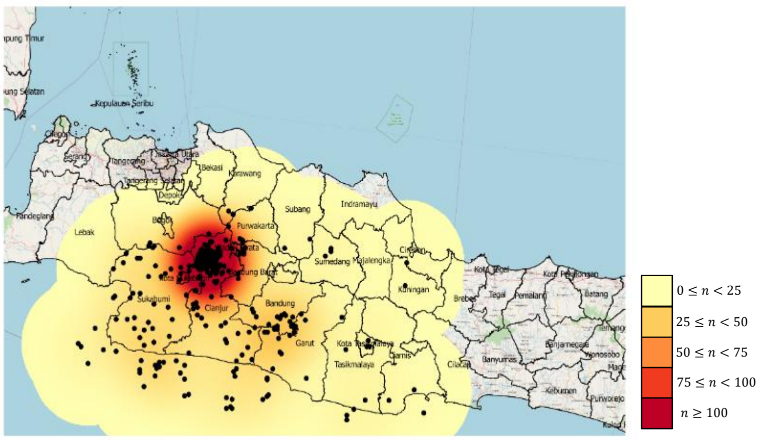

Figure 2. Visualization of the Spread of 2022 Earthquake Incidences in West Java.

The area with the highest number of earthquake points is Cianjur, which is marked in red on **Figure 2.**

3.2 Outlier Detection

Outliers are observations that are significantly different (extreme) from other observational data, thus it is necessary to detect outliers using a Boxplot.

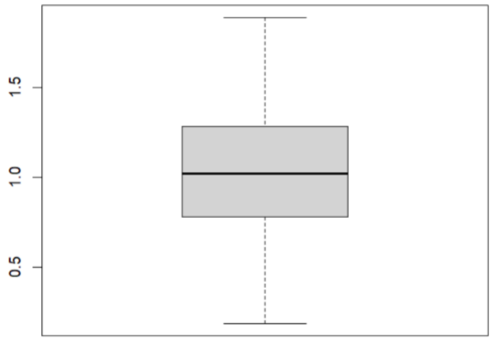

Figure 3. Outlier Detection Using a Boxplot

Figure 3 shows that the transformed earthquake magnitude data in West Java did not contain any outliers; therefore, further tests were performed. The data must be stationary to apply the ordinary kriging method. Data stationarity testing can be performed by creating a visualization as shown in **Figure 4**.

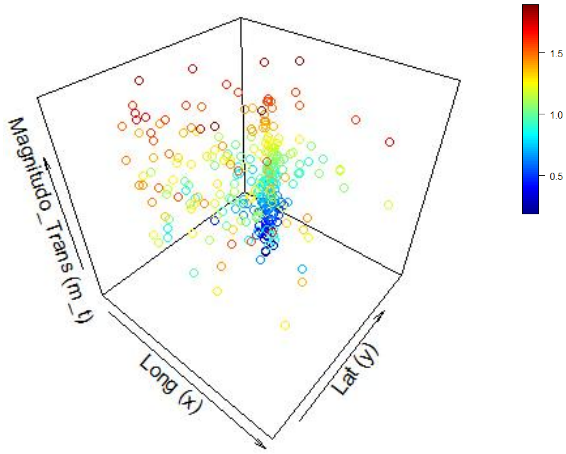

Figure 4. 3D Stationarity Plot of Earthquake Magnitude Data.

Figure 4 shows that the distribution pattern of the transformed earthquake magnitude data in West Java is randomly distributed, which is characterized by the colour of the randomly distributed points that does not appear dependent on a particular location, thus it can be concluded that the data is stationary.

3.3 Ordinary Kriging Estimation of Earthquake Magnitudes

To calculate semivariograms, the data were grouped into several classes using AutofitVariogram. The AutofitVariogram is an automatic process for estimating a variogram model that fits the given spatial data. The 247 training data, were divided into 12 classes.

Table 3. OK Experimental Semivariogram using *AutofitVariogram*.

Class	Number of Point Pairs	Average Distance (m)	Experimental Semivariogram
1	196	1353.67	0.080
2	840	3153.74	0.093
3	1186	5398.01	0.103
4	1791	8082.24	0.116
5	1547	11309.25	0.125
6	1077	14593.31	0.115
7	2425	21671.18	0.117
8	2277	32478.58	0.125
9	2997	46547.72	0.105
10	3418	63385.67	0.115
11	4545	79110.50	0.156
12	3502	97373.47	0.177

Semivariogram calculations can also be performed by grouping data into several classes using the Sturges approach, as shown in **Equation (7)**. This approach grouped the 247 training data into 9 classes.

Table 4. OK Semivariogram Experimental using Sturges

Class	Number of Point Pairs	Average Distance (m)	Experimental Semivariogram
1	10425	14468.91	0.114
2	6263	50341.80	0.111
3	7854	81781.73	0.161
4	3264	113585.60	0.149
5	1739	150036.10	0.169
6	511	182171.90	0.135
7	282	210678.00	0.097
8	39	250798.50	0.062
9	4	271403.50	0.021

3.4 Theoretical Semivariogram Analysis

Determining the theoretical semivariogram model requires the sill, nugget, and range parameter values. These parameters are obtained from AutofitVariogram through a process of trial-and-error process. The results of the AutofitVariogram obtained sill, nugget and range values of 0.12, 0.07, and 11451 Meters, respectively. After the trial-and-error process, a pair of parameters is selected for each theoretical semivariogram model based on the smallest MAPE value.

Table 5. Theoretical Semivariogram Parameter Values Obtained from the AutofitVariogram Function.

Model	Nugget	Sill	Range
Spherical	0.07	0.12	11451
Exponential	0.09	0.13	15000
Gaussian	0.09	0.19	15000

Table 6. Theoretical Semivariogram Parameter Values Obtained from the Sturges Method.

Model	Nugget	Sill	Range
Spherical	0.04	0.07	15000
Exponential	0.05	0.06	15000
Gaussian	0.06	0.16	11451

Structural analysis was used to determine the best theoretical semivariogram model. **Table 7** presents the error values for the three theoretical semivariogram models with the smallest MAPE value.

Table 7. Theoretical Semivariogram Error Values.

	Model	MAPE	MAE	RMSE
AutofitVariogram	Spherical	8.8100%	0.0124	0.0205
	Exponential	10.3120 %	0.0131	0.0185
	Gaussian	21.1360 %	0.0277	0.0349
Sturges	Spherical	61.5750 %	0.0545	0.0618
	Exponential	62.7640 %	0.0622	0.0701
	Gaussian	51.3530 %	0.0477	0.0586

Based on **Table 7**, the smallest MAPE, MAE, and RMSE values were achieved using the AutofitVariogram function on the Spherical model to estimate earthquake magnitude data in West Java in 2022.

3.5 Inverse Distance Weighting Estimation of Earthquake Magnitudes

In IDW interpolation, iteration is performed to determine the optimal power value which is selected from several power values based on the smallest MSE value. The iteration in this study used power values from 1 to 20 with an interval of 0.1.

Table 8. **MSE for Each Power Value.**

No	Power Value	Mean Squared Error (MSE)
1	1	0.3370548
2	1.1	0.3286231
⋮	⋮	⋮
11	1.9	0.2920265
12	2	0.2918020
⋮	⋮	⋮
200	20	0.3856330

The optimal power value was found to be $p = 2$ as it had the smallest MSE compared to other power values, with an MSE of 0.2918020 obtained from Leave One Out Cross Validation (LOOCV).

3.6 Best Method for Estimating Earthquake Magnitudes in West Java in 2022

The best method for estimating earthquake magnitude data in the West Java region is determined by analyzing the MAE and MAPE values.

Table 9. **Error Values from the IDW and OK Methods.**

Method	MAPE		MAE	
	Training	Testing	Training	Testing
Inverse Distance Weighting (IDW)	0.463	17.886	0.009	0.479
Ordinary Kriging (OK)	13.225	18.644	0.309	0.498

Based on the MAPE and MAE values, it was found that the IDW method attained a smaller error value than the OK method, therefore, it was used for the final estimation of earthquake magnitudes in the West Java region. Visualization of the interpolation results of 2022 earthquake magnitudes in West Java using the IDW method is presented in **Figure 5**.

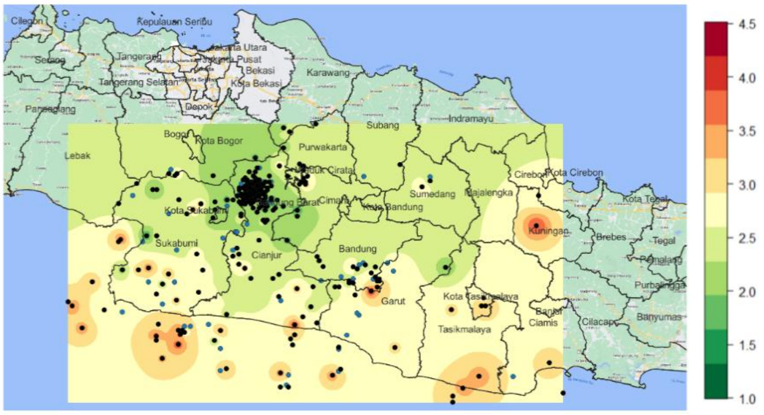

Figure 5. **Visualization of Earthquake Magnitude Interpolation Results**

The visualization in **Figure 5** suggests that a high magnitude earthquake has the potential to occur in the Kp. Cileuley, Garumukti, Pamulihan District, Garut Regency, West Java areas marked, which are marked in dark red. Meanwhile, the lowest estimated magnitudes are shown in dark green which may occur in the Kp Munjul, Munjul, Cianjur District, Cianjur Regency, West Java. From **Figure 5**, it is evident that the majority of the region falls within the 2.5 to 3 Richter scale range, indicating moderate but widespread seismic activity. The results in Figure 6 align with the geographical profile of West Java, which is located along both the Circum-Pacific and Mediterranean seismic belts. As a result, most of the area is considered geologically unstable, as indicated Thank you, we have revised it by the presence of seven active volcanoes, six active faults, and tectonic plate activity south of West Java. The complexity of the geological structure in this region increases its vulnerability to natural disasters **[28][29]**.

4. CONCLUSIONS

Smaller MAPE and MAE values indicate that the IDW method was more accurate at predicting the magnitude of the 2022 earthquakes in West Java in 2022 than the OK method with the best power value of 2. This research can help inform disaster mitigation plans for the government so that necessary actions can be taken to reduce disaster risks and ensure community safety. The majority of the region fell within the 2.5 to 5 Richter scale range, indicating moderate but widespread seismic activity. The results align with the geographical profile of West Java, which is located along both the Circum-Pacific and Mediterranean seismic belts. As a result, most of the area is considered geologically unstable, as indicated by the presence of seven active volcanoes, six active faults, and tectonic plate activity south of West Java.

ACKNOWLEDGMENT

The author would like to thank the Statistics Study Program, Faculty of Mathematics and Natural Sciences, Universitas Islam Indonesia for assisting in the research process.

REFERENCES

[1] Y. Syafitri, B. Bahtiar, and L. A. Didik, “ANALISIS PERGESERAN LEMPENG BUMI YANG MENINGKATKAN POTENSI TERJADINYA GEMPA BUMI DI PULAU LOMBOK,” *KONSTAN: Jurnal Fisika dan Pendidikan Fisika*, vol. 4, no. 2, pp. 139–146, Jan. 2020, doi: 10.20414/konstan.v4i2.43.

[2] A. W. S. R, J. Jasruddin, and N. Ihsan, “ANALISIS REKAHAN GEMPA BUMI DAN GEMPA BUMI SUSULAN DENGAN MENGGUNAKAN METODE OMORI,” *Jurnal Sains dan Pendidikan Fisika*, vol. 8, no. 3, pp. 263–268, 2012.

[3] Z. Zakaria, Ismawan, and I. Haryanto, “IDENTIFIKASI DAN MITIGASI PADA ZONA RAWAN GEMPA BUMI DI JAWA BARAT,” *Bulletin of Scientific Contribution*, vol. 9, no. 1, pp. 35–41, 2011.

[4] Badan Nasional Penanggualangan Bencana, MODUL TEKNISPENYUSUNAN KAJIAN RISIKO BENCANA GEMPA BUMI. Indonesia, 2019.

[5] A. T. Pradina and M. M. A. Pratama, “PENINGKATAN LITERASI MITIGASI BENCANA GEMPA BUMI MELALUI BOOKLET RINGKAS INOVATIF BAGI SISWA SDN WONOAYU KECAMATAN WAJAK KABUPATEN MALANG,” *Jurnal pasopati*, vol. 3, no. 3, pp. 168–176, 2021, [Online]. Available: http://ejournal2.undip.ac.id/index.php/pasopati

[6] D. F. Niode, Y. D. Y. Rindengan, and S. D. S. Karouw, “GEOGRAPHICAL INFORMATION SYSTEM (GIS) UNTUK MITIGASI BENCANA ALAM BANJIR DI KOTA MANADO,” *E-Journal Teknik Elektro dan Komputer*, vol. 5, no. 2, pp. 14–20, 2016.

[7] I. A. Ashari, R. A. Setiawan, and K. Nisa’, “IMPLEMENTASI WIRELESS SENSOR NETWORK: PERBANDINGAN METODE INVERSE DISTANCE WEIGHT DAN ORDINARY KRIGING UNTUK ESTIMASI KADAR GAS AMONIA PADA LINGKUNGAN PETERNAKAN,” *Jurnal Teknologi Informasi dan Ilmu Komputer*, vol. 9, no. 5, pp. 883–888, Oct. 2022, doi: 10.25126/jtiik.2022934394.

[8] M. C. Safira, A. Fauzan, and M. A. S. Adhiwibawa, “INTERPOLASI POLUTAN NITROGEN DIOKSIDA (NO2) DI KOTA YOGYAKARTA DENGAN PENDEKATAN ORDINARY KRIGING DAN INVERSE DISTANCE WEIGHTED,” *Jurnal Aplikasi Statistika & Komputasi Statistik*, vol. 14, no. 2, pp. 55–66, 2022.

[9] A. Sekulić, M. Kilibarda, G. B. M. Heuvelink, M. Nikolić, and B. Bajat, “RANDOM FOREST SPATIAL INTERPOLATION,” *Remote Sens (Basel)*, vol. 12, no. 10, p. 1687, May 2020, doi: 10.3390/rs12101687.

[10] Q. Hu, Z. Li, L. Wang, Y. Huang, Y. Wang, and L. Li, “RAINFALL SPATIAL ESTIMATIONS: A REVIEW FROM SPATIAL INTERPOLATION TO MULTI-SOURCE DATA MERGING,” *Water (Basel)*, vol. 11, no. 3, p. 579, Mar. 2019, doi: 10.3390/w11030579.

[11] Q. M. Ajaj, M. A. Shareef, N. D. Hassan, S. F. Hasan, and A. M. Noori, “GIS BASED SPATIAL MODELING TO MAPPING AND ESTIMATION RELATIVE RISK OF DIFFERENT DISEASES USING INVERSE DISTANCE WEIGHTING (IDW) INTERPOLATION ALGORITHM AND EVIDENTIAL BELIEF FUNCTION (EBF)(CASE STUDY: MINOR PART OF KIRKUK CITY, IRAQ),” *Int. J. Eng. Technol*, vol. 7, no. 4, pp. 185–191, 2018.

[12] B. N. Ruchjana, A. N. Falah, and A. S. Abdullah, “APPLICATION OF THE ORDINARY KRIGING METHOD FOR PREDICTION OF THE POSITIVE SPREAD OF COVID-19 IN WEST JAVA,” *J Phys Conf Ser*, vol. 1722, no. 1, p. 012026, Jan. 2021, doi: 10.1088/1742-6596/1722/1/012026.

[13] T. Gia Pham, M. Kappas, C. Van Huynh, and L. Hoang Khanh Nguyen, “APPLICATION OF ORDINARY KRIGING AND REGRESSION KRIGING METHOD FOR SOIL PROPERTIES MAPPING IN HILLY REGION OF CENTRAL VIETNAM,” *ISPRS Int J Geoinf*, vol. 8, no. 3, p. 147, Mar. 2019, doi: 10.3390/ijgi8030147.

[14] P. Qiao, M. Lei, S. Yang, J. Yang, G. Guo, and X. Zhou, “COMPARING ORDINARY KRIGING AND INVERSE DISTANCE WEIGHTING FOR SOIL AS POLLUTION IN BEIJING,” *Environmental Science and Pollution Research*, vol. 25, no. 16, pp. 15597–15608, Jun. 2018, doi: 10.1007/s11356-018-1552-y.

[15] P. Kumar, B. Rao, A. Burman, S. Kumar, and P. Samui, “SPATIAL VARIATION OF PERMEABILITY AND CONSOLIDATION BEHAVIORS OF SOIL USING ORDINARY KRIGING METHOD,” *Groundw Sustain Dev*, vol. 20, p. 100856, Feb. 2023, doi: 10.1016/j.gsd.2022.100856.

[16] A. Lamamra, D. L. Neguritsa, and M. Mazari, "GEOSTATISTICAL MODELING BY THE ORDINARY KRIGING IN THE ESTIMATION OF MINERAL RESOURCES ON THE KIESELGUHR MINE, ALGERIA," *IOP Conf Ser Earth Environ Sci*, vol. 362, no. 1, p. 012051, Nov. 2019, doi: 10.1088/1755-1315/362/1/012051.

[17] E. Kostopoulou, "APPLICABILITY OF ORDINARY KRIGING MODELING TECHNIQUES FOR FILLING SATELLITE DATA GAPS IN SUPPORT OF COASTAL MANAGEMENT," *Model Earth Syst Environ*, vol. 7, no. 2, pp. 1145–1158, Jun. 2021, doi: 10.1007/s40808-020-00940-5.

[18] R. Yendra and R. R. Risman, "PENERAPAN METODE ORDINARY KRIGING PADA PENDUGAAN KRIMINALITAS DI KOTA PEKANBARU RIAU," *Jurnal Sains Matematika dan Statistika*, vol. 5, no. 1, 2019.

[19] G. Rozalia, H. Yasin, and D. Ispriyanti, "PENERAPAN METODE ORDINARY KRIGING PADA PENDUGAAN KADAR NO2 DI UDARA (STUDI KASUS: PENCEMARAN UDARA DI KOTA SEMARANG)," *Jurnal Gaussian*, vol. 5, no. 1, pp. 113–121, 2016, [Online]. Available: http://ejournal-s1.undip.ac.id/index.php/gaussian

[20] N. L. Humairah and A. Fauzan, "SPATIAL INSIGHTS INTO EARTHQUAKE STRENGTH: A SULAWESI CASE STUDY USING ORDINARY AND ROBUST KRIGING METHODS," *BAREKENG: Jurnal Ilmu Matematika dan Terapan*, vol. 18, no. 2, pp. 1283–1296, May 2024, doi: 10.30598/barekengvol18iss2pp1283-1296.

[21] K. Krivoruchko, "EMPIRICAL BAYESIAN KRIGING IMPLEMENTED IN ARCGIS GEOSTATISTICAL ANALYST," 2012.

[22] R. T. Oktaviani, "CARBON MONOOXIDE (CO) ESTIMATION OF AIR POLLUTION IN SURABAYA USING UNIVERSAL KRIGING METHOD," Final Task, Institut Teknologi Sepuluh Nopember, Surabaya, 2015.

[23] G. Rozalia, H. Yasin, and D. Ispriyanti, "PENERAPAN METODE ORDINARY KRIGING PADA PENDUGAAN KADAR NO 2 DI UDARA (STUDI KASUS: PENCEMARAN UDARA DI KOTA SEMARANG)," *Jurnal Gaussian*, vol. 5, no. 1, pp. 113–121, 2016, [Online]. Available: http://ejournal-s1.undip.ac.id/index.php/gaussian

[24] E. Respatti, R. Goejantoro, and S. Wahyuningsih, "COMPARISON OF ORDINARY KRIGING AND INVERSE DISTANCE WEIGHTED METHODS FOR ESTIMATION OF ELEVATIONS USING TOPOGRAPHIC DATA (CASE STUDY: FMIPA UNIVERSITY OF MULAWARMAN'S TOPOGRAPHIC)," *Jurnal EKSPONENSIAL*, vol. 5, no. 2, pp. 163–170, 2014.

[25] J. M. Pasaribu, N. Suryo, H. P. Pemanfaatan, and P. Jauh, "COMPARISON OF DEM SRTM INTERPOLATION TECHNIQUES USING INVERSE DISTANCE WEIGHTED (IDW), NATURAL NEIGHBOR AND SPLINE METHOD," *Jurnal Penginderaan Jauh*, vol. 9, no. 2, pp. 126–139, 2012.

[26] H. Purnomo, "APLIKASI METODE INTERPOLASI INVERSE DISTANCE WEIGHTING DALAM PENAKSIRAN SUMBERDAYA LATERIT NIKEL (STUDI KASUS DI BLOK R, KABUPATEN KONAWE-SULAWESI TENGGARA)," *Jurnal Ilmiah Bidang Teknologi, ANGKASA*, vol. x, no. 1, pp. 49–60, 2018.

[27] E. Woschnagg and J. Cipan, EVALUATING FORECAST ACCURACY. University of Vienna, 2004.

[28] Badan Nasional Penanggulangan Bencana, KAJIAN RISIKO BENCANA NASIONAL PROVINSI JAWA BARAT 2022-2026. Indonesia, 2021.

[29] I. Haryanto, E. Sukiyah, N. N. Ilmi, Y. A. Sendajaja, and E. Sunardi, "TECTONICS ACTIVITY AND VOLCANISM INFLUENCE TO THE GARUT AND LELES BASINS CONFIGURATION AND THE IMPLICATION ON ENVIRONMENTAL GEOLOGY," *International Journal of Science and Research (IJSR)*, vol. 6, no. 1, pp. 2287–2292, Jan. 2017, doi: 10.21275/art20164646.